MASTER THESIS

Development of beam elements composed of timber and steel for medium-rise office buildings considering fire safety

submitted for the akademic degree of
Master of Science

under the direction of
Prof. DDI Wolfgang Winter

E 259/2
Institute of Architectural Sciences
Structural Design and Timber Engineering

by

DI Bunji Izumi

0527257

Ferrogasse 43/11

A1180 Wien

Vienna, Austria on 16th September 2008

Contents

List of Figures

List of Tables

Chapter 1

Introduction

1.1 Background

The number of the application of medium-rise multi-story wood buildings has been increasing. In west European countries, such as United Kingdom, Switzerland, Sweden and Austria. Timber itself is a good medium of CO2 stock. Therefore, it is assumed that the urban area has the potential to be a huge CO2 stock when the application of timber-derived structure is widened. In the urban area, most of the buildings have multistory floors and by now, the knowledge has been accumulated in the field of middle-rise multistory buildings made of timber.

Figure 1.1 is an image of the wooden structure which is so far considered to be the oldest in the world. The building was build in the 7th century, and it has experienced several disasters and major restorations. According to Larsen, et al, it has gone through at least three complete dismantle-repair-reassemble restoration (in 1374, 1603 and the beginning of 20th century) and the percentage of original wooden members nowadays is estimated to be no more than 15-20 percent [12]. This case shows the way how timber structure can be conserved through centuries. Although this is one of the extreme cases, the idea of "replaceablity of (structural) members" can be introduced to modern buildings made of timber, even though whose period in service will not be supposed to be more than a century.

The major threats against timber structure are those derived from insects and fungi. The author thinks it ideal for the timber structure to be exposed to the air, in order not only to let the structure expose to the air and release the humidity but also for the users of the building to detect the damaged area immediately.

In the architectural planning, on the other hand, it is often the case that a building has its structure inside of a wall. Figure 1.2 shows one of a typical wall compositions with fire resistance category REI60, with which I would like to change the situation. The concept of this kind of composition is the integration among separation wall (=architectural planning), structural element, thermal isolation and fire protection. One of the disadvantages of this system lies in the point that it is hard to detect what is happening in the wall.

Figure 1.1: The Golden Hall, Horyu-ji Temple [1]

[1] image cited from http://http://upload.wikimedia.org/wikipedia/commons/1/17/Horyu-ji11s3200.jpg
protected with GFDL and CreativeCommons 2.5 by 663highland

Since it was allowed to build multi-story timber buildings, the issue of fire protection has been gaining importance. There are several methods available for applying to timber structures.

1.2 Purpose

In this research, in order to increase the ways of application of timber to buildings, the target is set to create a structural system which is composed of timber and steel. As frame structure is more common in high-rise buildings, the system targets to apply to tall buildings which have more than 5 stories.

The building physics issue is not within the scope of this research, and is discussed only qualitatively.

1.3 Method and Structure

In this research, in the following chapter, the past researches of each field is summarized. In chapter 3, the structural element which has fire resistant property is developed. The structural development is summarized in Chapter 4.

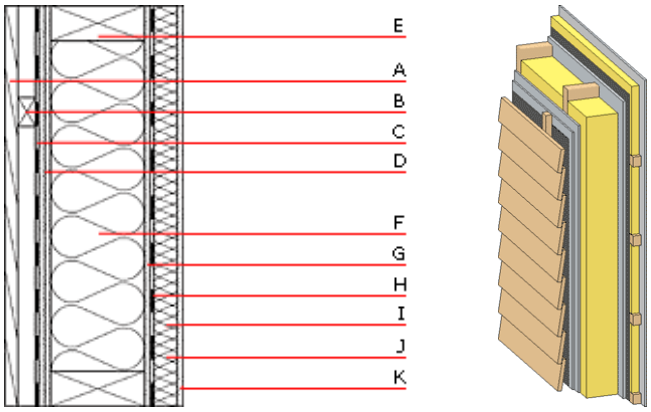

(a) t=3600 (b) t=14400

Figure 1.2: Example of contemporary structure, from DATAHOLZ Website, http://dataholz.com

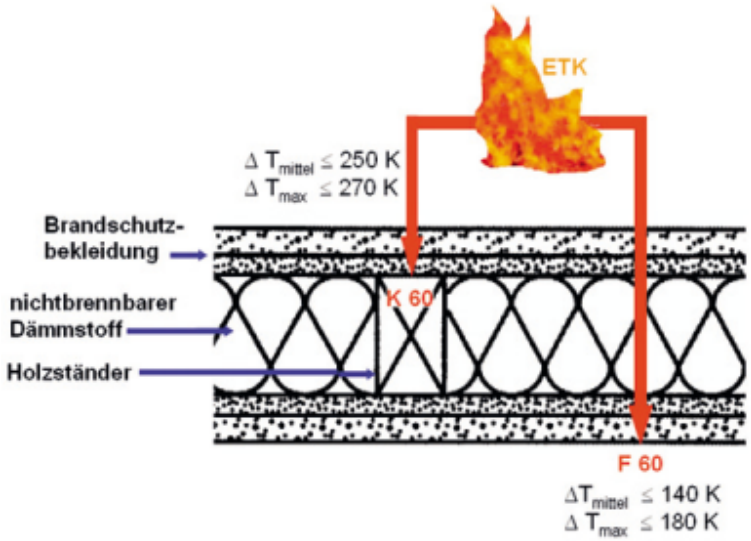

Figure 1.3: Fire protection concept, drawing extracted from [8]

Chapter 2

Past Researches of the fields

2.1 Fire protection

2.1.1 H-shaped beam embedded in glued laminated timber

Building Research Institute in Japan (BRI) conducted a series of combustion tests in 2003 [9] within the frame of development of technologies of timber composite structures. The typical geometry of the test was composed of glued laminated timber of various species and H-shaped steels which were embed in the timber. The combustion tests were conducted with the scenario which were composed of 60 minutes' heating phase and subsequent 3 hours' observation period without heating.

2.1.2 Mortar piece embedded in glued laminated timber

Oka, et al [13] developed structural hybrid elements for frame system, which is composed of timber (Japanese cider) and mortar pieces. Japanese cider is considered to be the species which is the lowest in fire-resistant property. They proposed several sections for beam and column elements, and conducted combustion tests. They introduced the three layers of different function to their elements. Those are, (i) surface layer, (ii) self-extinguishing layer, and (iii) load-bearing layer.

2.2 Integration of structural and fire-protective design

Figure 2.2 is the image of the building which the author designed for National University of Kaohsiung in Taiwan, in his master thesis[10] in Vienna University of Technology. The building was designed, employing timber-steel hybrid beams and columns. The element was designed which he developed in terms of structural and fire-resistant properties. By hiring the experimental results of combustion tests of timber-steel hybrid sections from BRI Japan in 2003, he developed and calibrated the two-dimensional thermal finite element analysis tool. Using the simulation tool,

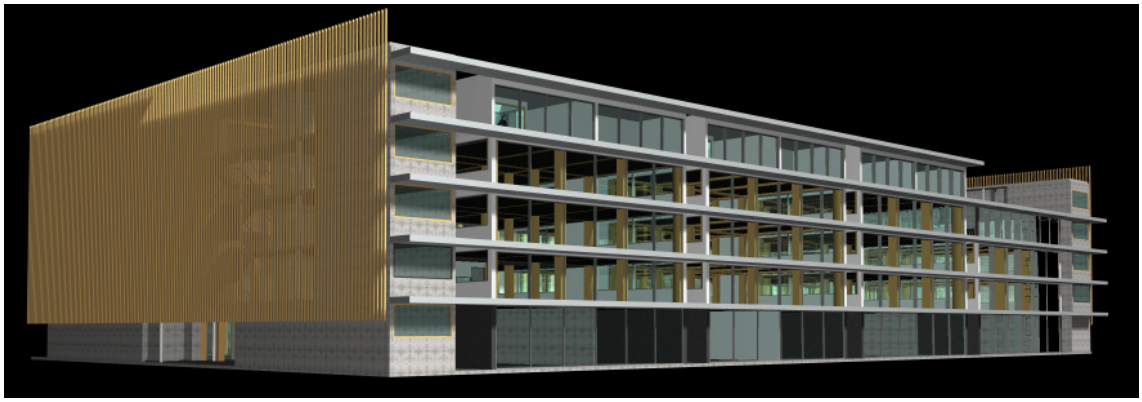

Figure 2.1: Proposed building in National University of Kaohsiung

he proposed several possible sections for beam and column, and the section properties before and after a fire event with 60 minutes' heating phase and subsequent 3 hours' observation period without heating were investigated.
The previous research by the author has been revealed the possibility of timber-steel hybrid structure, yet the structural properties of the elements has not been surveyed in detail. Therefore the scope within this research is set on the structural behavior of the hybrid sections, especially for beams.

Chapter 3

Thermal simulation

3.1 Theoretical background of transient heat transfer

3.1.1 Transient heat transfer

Theory of conduction heat transfer was applied for the analysis. In this section, Derivations and evolutions of equations are based upon the reference [7].

Conduction heat transfer is one of three ways for the heat transmission, and it is dominant when the heat is transmitted through the solid bodies. Heat energy transfers from the area with higher temperature to lower temperature. when q describes the amount of heat which is transmitted per unit time period, and per unit area,

$$q = -\lambda A \frac{\partial T}{\partial x} \tag{3.1}$$

where the proportionality factor λ is called thermal conductivity.

From the energy balance, following equation comes into existence:

$$\text{(heat income)} = \text{(heat emission)} + \text{(change in internal energy)} \tag{3.2}$$

where the change of internal energy of micro area is described as follows:

$$\text{(change of internal energy)} = \rho c A \frac{\partial T}{\partial t} dx \tag{3.3}$$

Above is the one-dimensional conduction heat transfer equation. When the system is three-dimensional, the equation of the energy balance (without heat generation) is described as follows:

$$q_x + q_y + q_z = q_{x+dx} + q_{y+dy} + q_{z_d z} + \frac{dE}{dt} \tag{3.4}$$

where

$$\frac{dE}{dt} = \rho c dx dy dz \frac{\partial T}{\partial t} \tag{3.5}$$

Therefore, the general form of three-dimensional conduction heat transfer equation is expressed as follows, deploying Eq.(3.4)

$$\frac{\partial}{\partial x}\left(\lambda\frac{\partial T}{\partial x}\right)+\frac{\partial}{\partial y}\left(\lambda\frac{\partial T}{\partial y}\right)+\frac{\partial}{\partial z}\left(\lambda\frac{\partial T}{\partial z}\right)=\rho c\frac{\partial T}{\partial t} \tag{3.6}$$

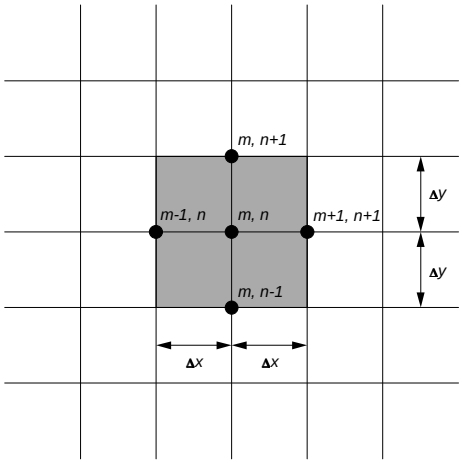

Figure 3.1: Two-dimensional thermal transient analysis, extracted from [7], redrawn by the author

3.1.2 Numerical analytical method

Figure 3.1.2 shows two-dimensional thermal system. Differential equation is as follows:

$$\lambda \left(\frac{\partial^2 T}{\partial x^2} + \frac{\partial^2 T}{\partial y^2} \right) = \rho c \frac{\partial T}{\partial t} \tag{3.7}$$

The partial derivatives can be approximated as follows:

$$\frac{\partial^2 T}{\partial x^2} \approx \frac{1}{(\Delta x)^2} \left(T_{m+1,n} + T_{m-1,n} - 2T_{m,n} \right) \tag{3.8}$$

$$\frac{\partial^2 T}{\partial y^2} \approx \frac{1}{(\Delta y)^2} \left(T_{m,n+1} + T_{m,n-1} - 2T_{m,n} \right) \tag{3.9}$$

$$\frac{\partial T}{\partial t} \approx \frac{{T_{m,n}}^{p+1} - {T_{m,n}}^{p}}{(\Delta t)} \tag{3.10}$$

From Equation (3.7) to Equation (3.10), the difference equation is developed as follows:

$$\frac{{T_{m+1,n}}^{p} + {T_{m-1,n}}^{p} - 2{T_{m,n}}^{p}}{(\Delta x)^2} + \frac{{T_{m,n+1}}^{p} + {T_{m,n-1}}^{p} - 2{T_{m,n}}^{p}}{(\Delta y)^2} = \frac{1}{\alpha} \frac{{T_{m,n}}^{p+1} - {T_{m,n}}^{p}}{(\Delta t)} \tag{3.11}$$

In Equation 3.11, α is defined as thermal diffusivity.

$$\alpha = \frac{\lambda}{\rho c} \tag{3.12}$$

Thermal diffusivity α indicates the diffusing speed of heat. In Equation 3.11, the relationship between temperatures of a certain point at time p and time $p+1$ is described. This means, when temperature of each point at time p (possibly the initial temperature) is known, that at time $p+1$ can be obtained.

3.2 Simple prediction method

A hypothesis was developed, in order to estimate the degree of improvement in the performance against fire. From a distant view where the beam is treated as one body, i.e. when the geometrical configuration of timber and steel in the sections is ignored, the body is treated as a thermal mass with certain heat content, depending on the volumetric ratios of timber and steel, or other materials.

As the value for specific heat of materials varies depending on temperature, the values at 200 °C were taken in order to remain the problem simple. Specific heat for steel at 200°C is set to 531.87 [J/kg·K] which is obtained by interpolating the given values (Table 3.5) in the reference[9]. Summary of the taken values is shown in Table 3.5.

Table 3.1: Applied material properties at 200°C

	steel	timber
Density ρ [kg/m^3]	7857	375
Thermal conductivity λ [W/m·K]	45	0.150
Specific heat c [J/kg·K]	531.87	2000

When the materials are applied to the elements of building construction, the value of ρc ([J/m^3 ·K])is more convenient to evaluate the thermal performance of the element compared to c, when it is assumed that the area of cross-sections are decided by the structural performance and does not vary much. Table 3.2 indicates that the same amount of steel has ca. 5.6 times as high thermal capacity as timber has.

Table 3.2: ρc values at 200°C

	steel	timber
ρc [kJ/m^3·K]	4178.9	750.00

3.3 Comparison between simplified method and two dimensional finite element method

3.3.1 Overview

Simplified method to predict the thermal performance of the section has been proposed in the previous section. In this section, the method is applied to several column and beam cross-sections and the results are compared.

3.3.2 Two-dimensional thermal sections

Four column sections, including timber solid section were extracted from the previous research by the author [10]. The geometries of the sections are shown in Figure 3.2 and 3.3

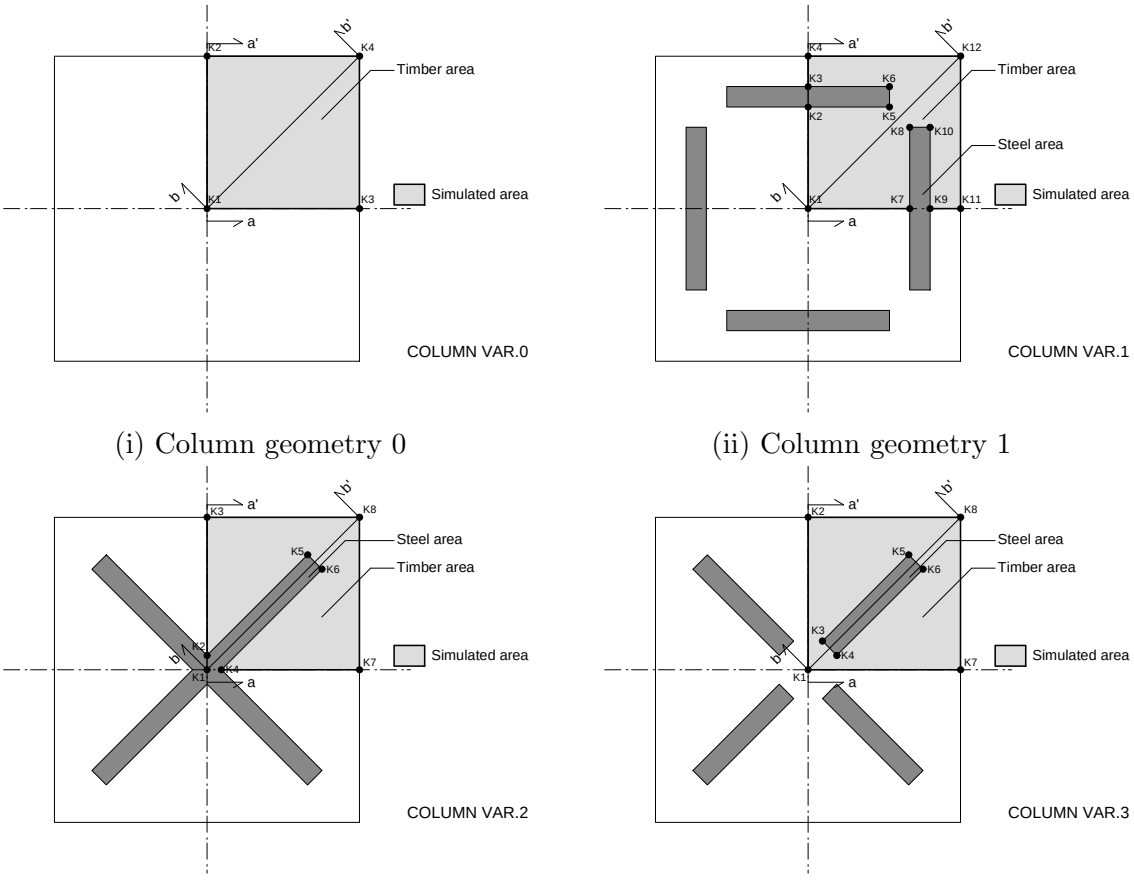

(i) Column geometry 0

(ii) Column geometry 1

(iii) Column geometry 2

(iv) Column geometry 3

Figure 3.2: Column geometries

Table 3.3: The coordinates of the specimens (columns)

	VAR.1	VAR.2	VAR.3
K1	(0,0)	(0,0)	(0,0)
K2	(0,100)	(0,14.1)	(0,150)
K3	(0,120)	(0,150)	(14.1,28.3)
K4	(0,150)	(14.1,0)	(28.3,14.1)
K5	(80,100)	(99.0,113.1)	(99.0,113.1)
K6	(80,120)	(113.1,99.0)	(113.1,99.0)
K7	(100,0)	(150,0)	(150,0)
K8	(100,80)	(150,150)	(150,150)
K9	(120,0)		
K10	(120,80)		
K11	(150,0)		
K12	(150,150)		

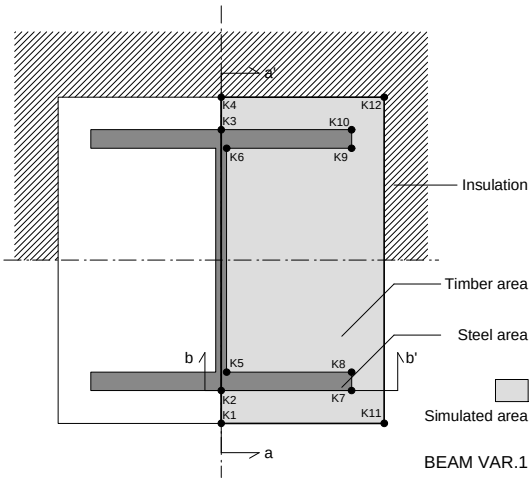

(i) Beam geometry 1

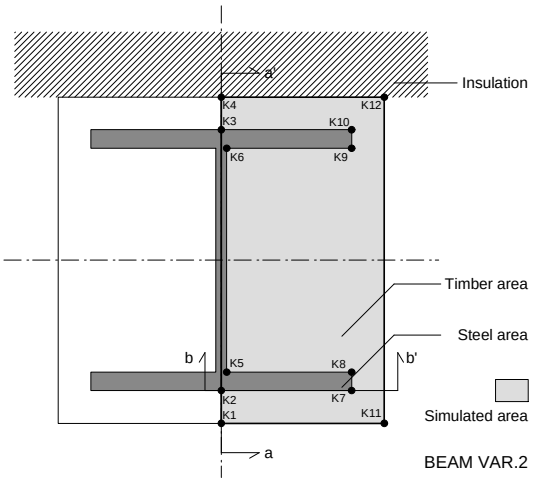

(ii) Beam geometry 2

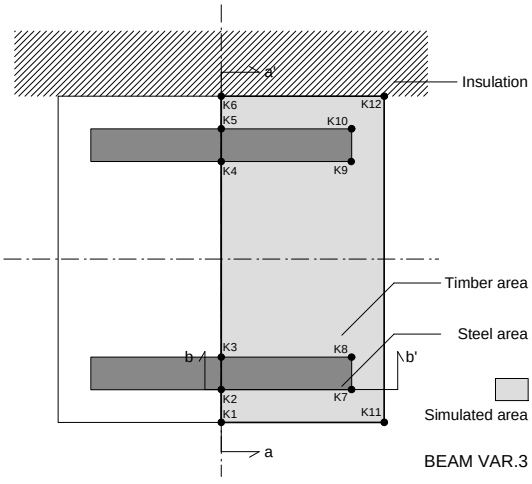

(iii) Beam geometry 3

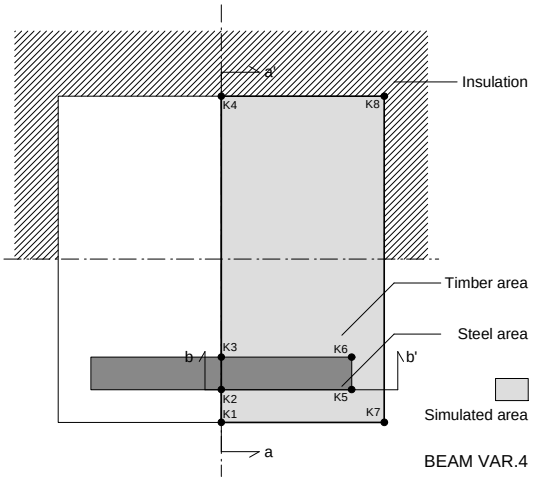

(iv) Beam geometry 4

Figure 3.3: Beam geometries

Table 3.4: The coordinates of the specimens (beams)

	VAR.1 , VAR.2	VAR.3	VAR.4
K1	(0,0)	(0,0)	(0,0)
K2	(0,30)	(0,30)	(0,30)
K3	(0,270)	(0,60)	(0,60)
K4	(0,300)	(0,240)	(0,300)
K5	(3.75,42)	(0,270)	(120,30)
K6	(3.75,258)	(0,300)	(120,60)
K7	(115,30)	(120,30)	(150,0)
K8	(115,42)	(120,60)	(150,300)
K9	(115,258)	(120,240)	
K10	(115,270)	(120,270)	
K11	(150,0)	(150,0)	
K12	(150,300)	(150,300)	

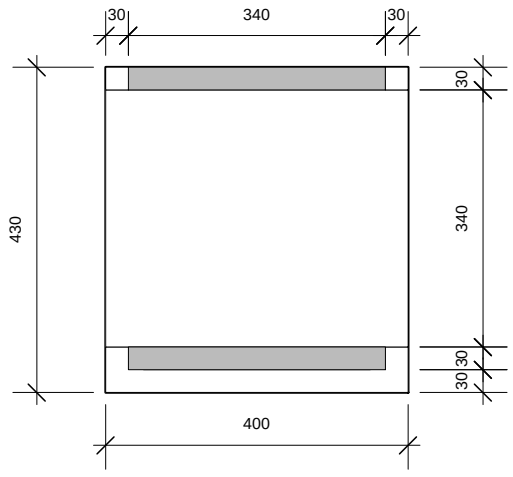

Figure 3.4: Section for thermal analysis

3.4 Three-dimensional finite element analysis of beam elements

3.4.1 Introduction

In order to survey the transition of temperature distribution in the cross sections, thermal transient finite element analysis was conducted. The conduction heat transfer was respected, and the temperature as a function of time, $T(t)$, was attached directly to the original surface of the cross sections.

Table 3.5: Material properties of steel

	300[K]	600[K]
Density [kg/m^3]	7920	7810
Thermal conductivity [W/m·K]	45	45
Specific heat [J/kg·K]	499	556

Table 3.6: Temperature-thermal conductivity relationship for wood and the char layer [5]

Temperature [°C]	Thermal conductivity [W/(m · K)]
20	0.12
200	0.15
350	0.07
500	0.09
800	0.35
1200	1.50

3.4.2 Material properties of timber

The material properties of timber were selected from those in EN 1995-1-2[5].

Thermal conductivity Instead of modeling the crack which appears after 500 $°C$, the effect of cracks was input by giving the increased value in thermal conductivity. The recommended value in EN 1995-1-2 includes the effect of penetrating heat flux after 500 $°C$, and consumption of charred layer after 1000 $°C$. The taken values and its graph are shown in Table 3.6 and Figure 3.5 respectively.

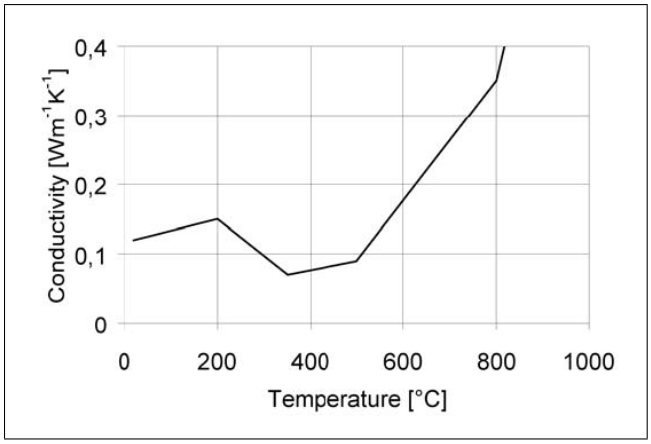

Figure 3.5: Temperature-thermal conductivity relationship for wood and the char layer, extracted from [5]

Specific heat As is the same with effect of cracks in thermal conductivity, the effect of latent heat around 100 $°C$ was included in specific heat. Table 3.7 shows the recommended value in EN 1995-1-2 [5].

Density In EN 1995-1-2, density is described by the ratio when that in 120 $°C$ is set to 1.00. The ratio is shown in Figure 3.7 and Table.

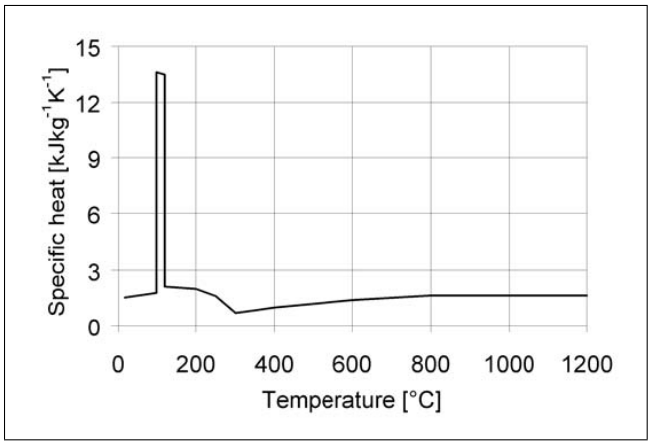

Figure 3.6: Temperature-specific heat relationship for wood and charcoal, extracted from [5]

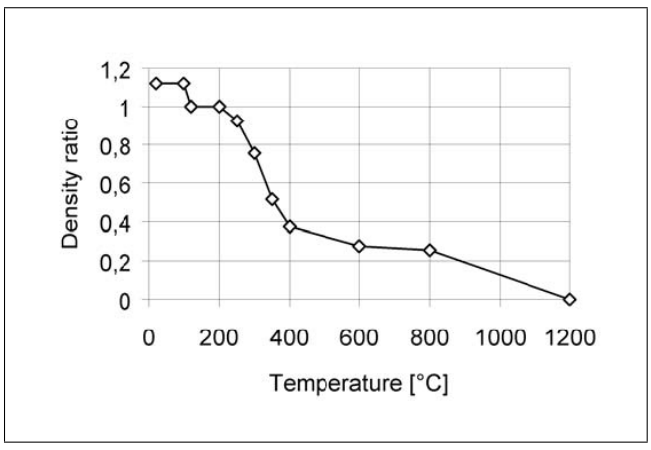

Figure 3.7: Temperature-density ratio for softwood with an initial moisture content of 12 % , extracted from [5]

Table 3.7: Temperature-specific heat relationship for wood and charcoal [5]

Temperature [°C]	Specific heat capacity [kJ/(kg · K)]
20	1.53
99	1.77
99	13.60
120	13.50
120	2.12
200	2.00
250	1.62
300	0.71
350	0.85
400	1.00
600	1.40
800	1.65
1200	1.65

Table 3.8: Temperature-density relationship for wood and charcoal [5]

Temperature [°C]	Density ratio [1]
20	1+ω
99	1+ω
99	1+ω
120	1.00
120	1.00
200	1.00
250	0.93
300	0.76
350	0.52
400	0.38
600	0.28
800	0.26
1200	0

[1] ω is the moisture content

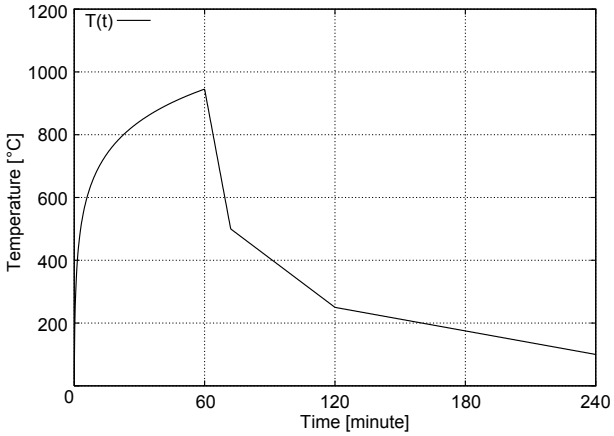

Figure 3.8: Input temperature

3.4.3 Fire scenario

Fire scenario was employed from the experimental result of the combustion test in Building Research Institute in Japan[9]. The temperature curve over time is shown in Figure fig:iso834. It has 60 minutes' heating face which follows along standard heating curve ISO 834, with subsequent 3 hours' "observation" period in the oven without heating.

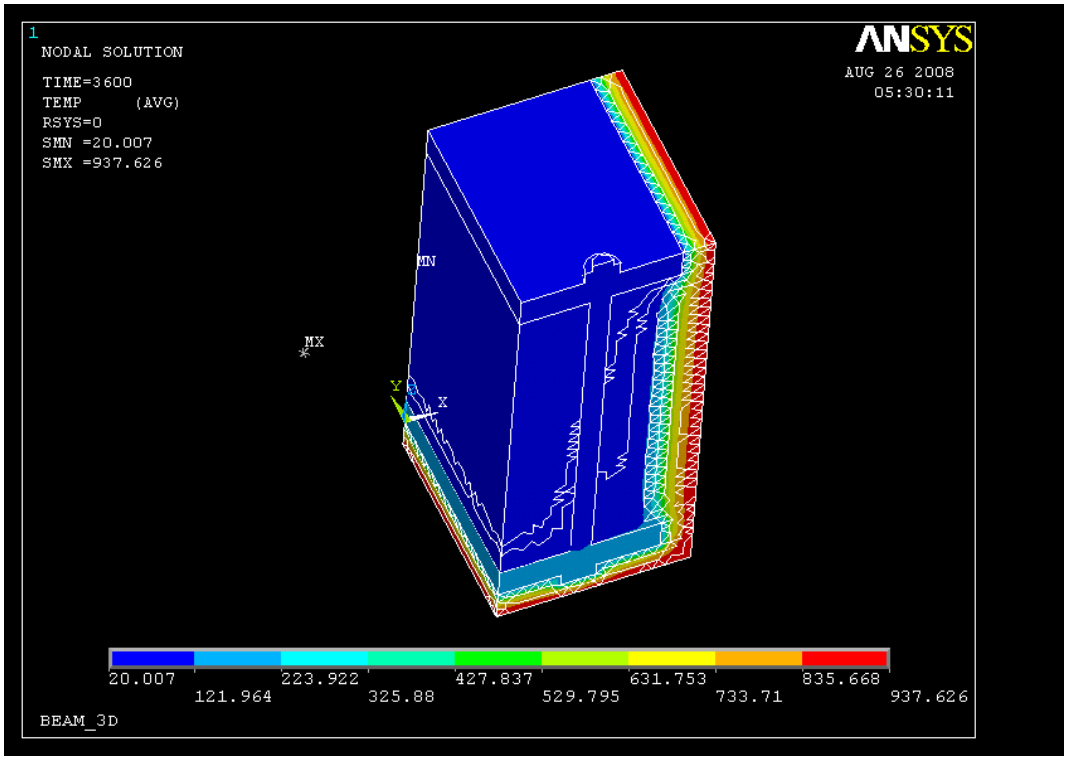

Figure 3.9: Temperature distribution at 3600[S]

3.4.4 Geometry

In the previous research by the author [10] [11], the two-dimensional thermal simulation has already been carried out with the same material properties and fire scenario. It has been proved already by several researchers [3, 9, 11] including the author, that steel embed in the timber cross-section is effective in reducing the charring velocity of timber. It is assumed that the increased heat capacity contributes to this phenomena. Another advantage of steel is that it has 300 times as high thermal conductivity as timber does. On the other hand, when they are compared per unit volume, steel has about 5.6 times as high thermal capacity as timber has, as has been discussed in Section 3.2.

3.4.5 Simulation Result

Simulations with two geometries were carried out. The geometries are shown in Figure X.(on going)

Geometry variant 1

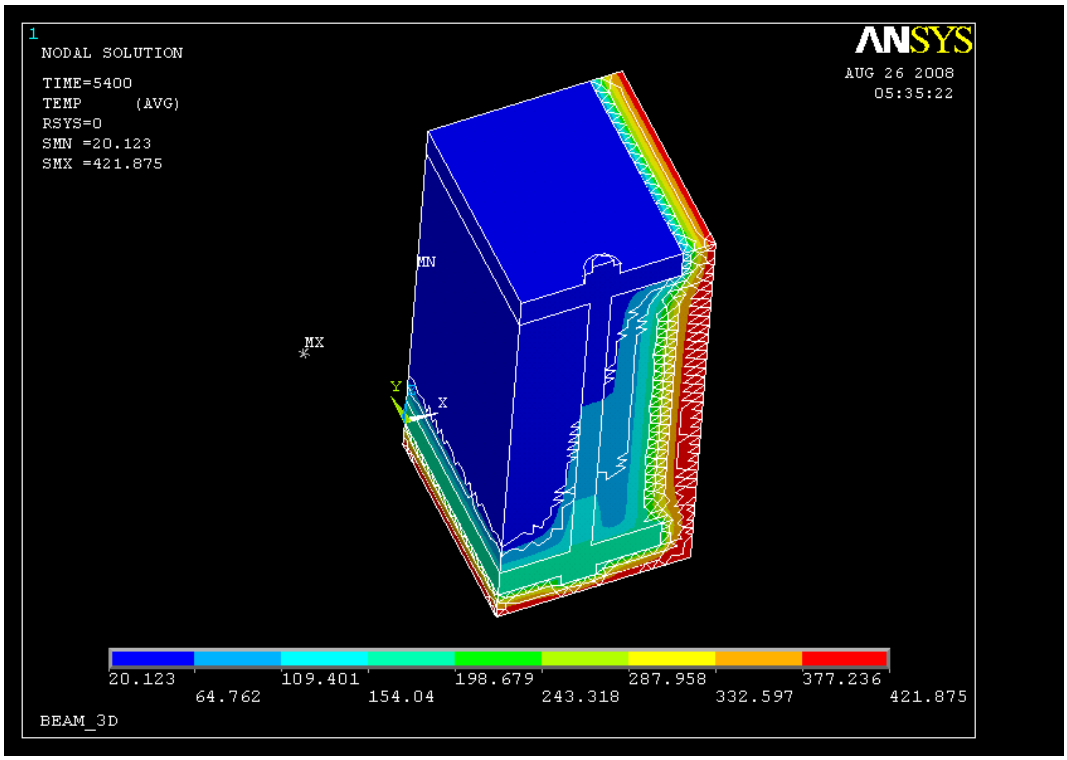

Figure 3.10: Temperature distribution at 5400[S]

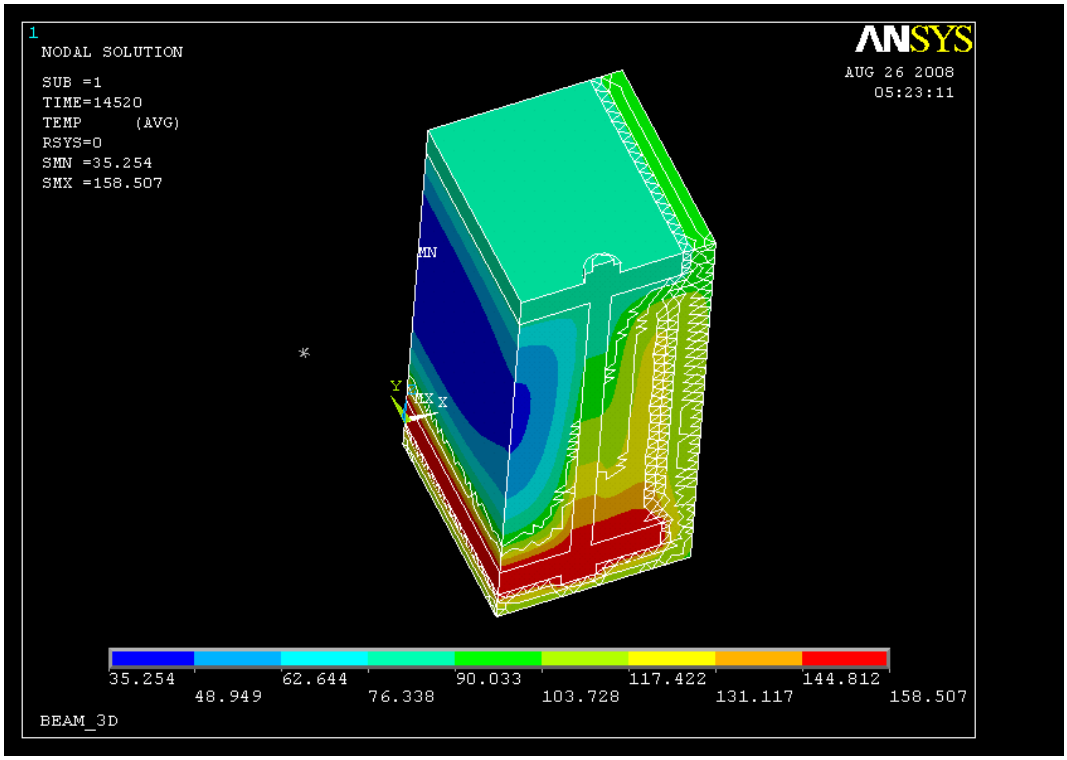

Figure 3.11: Temperature distribution at 14400[S]

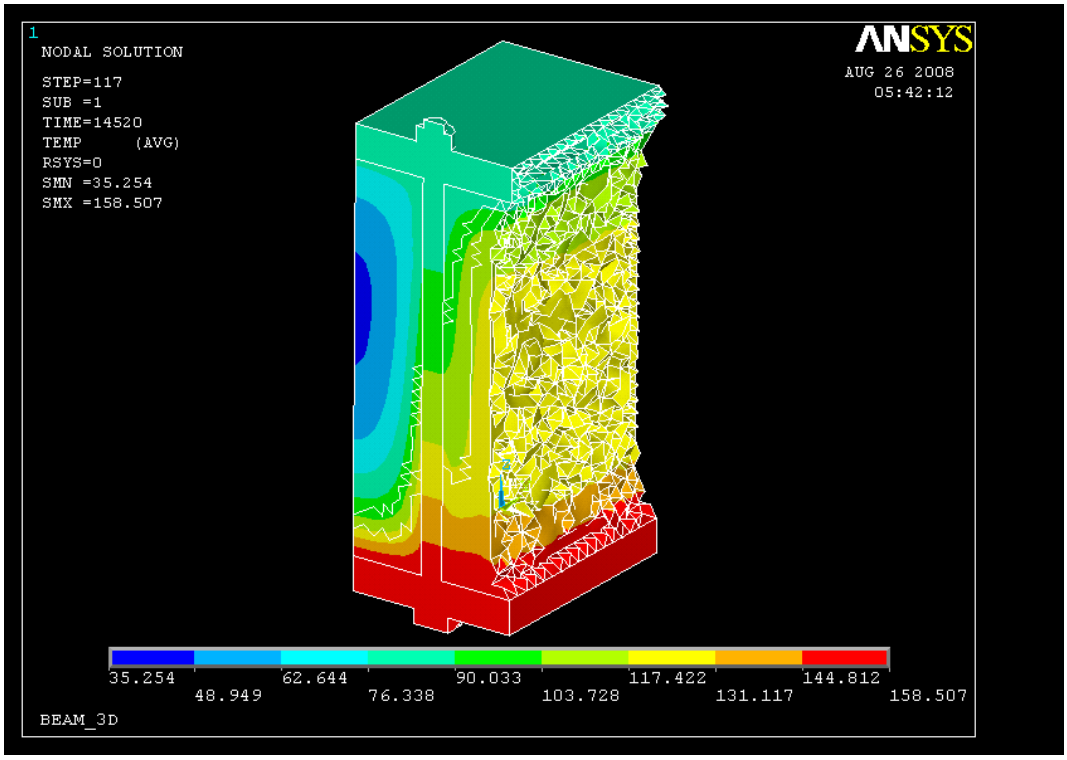

Figure 3.12: Remaining section at 14400[S]

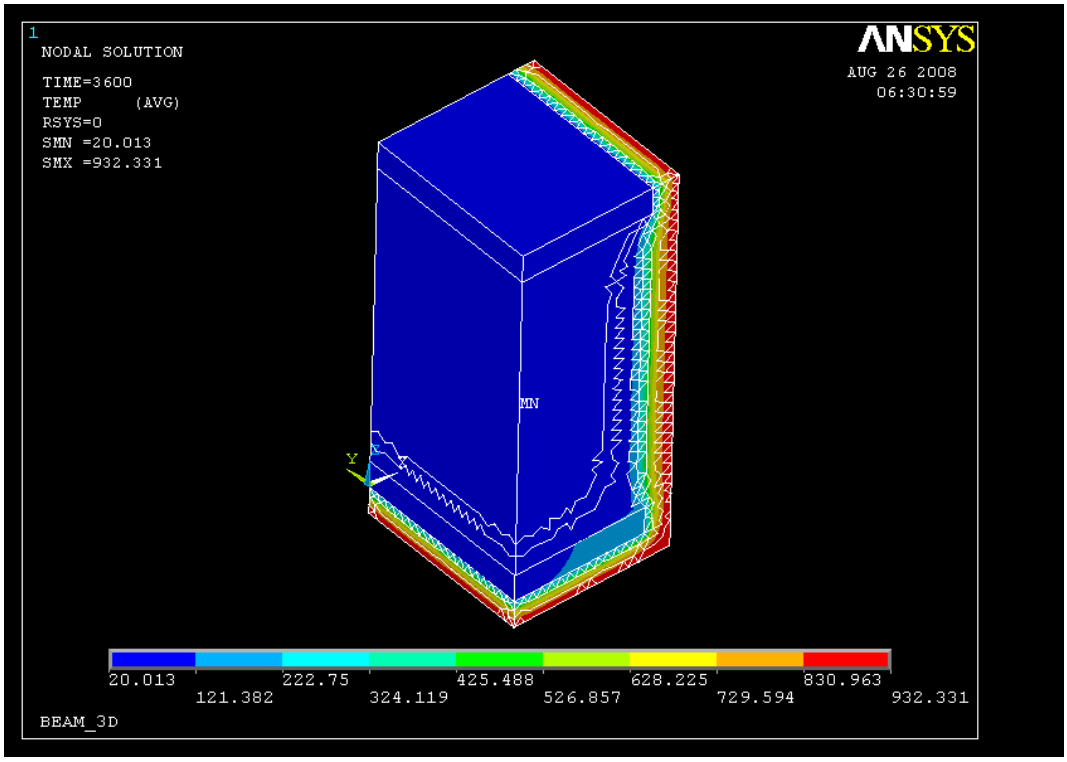

Figure 3.13: Temperature distribution at 3600[S]

Geometry variant 2

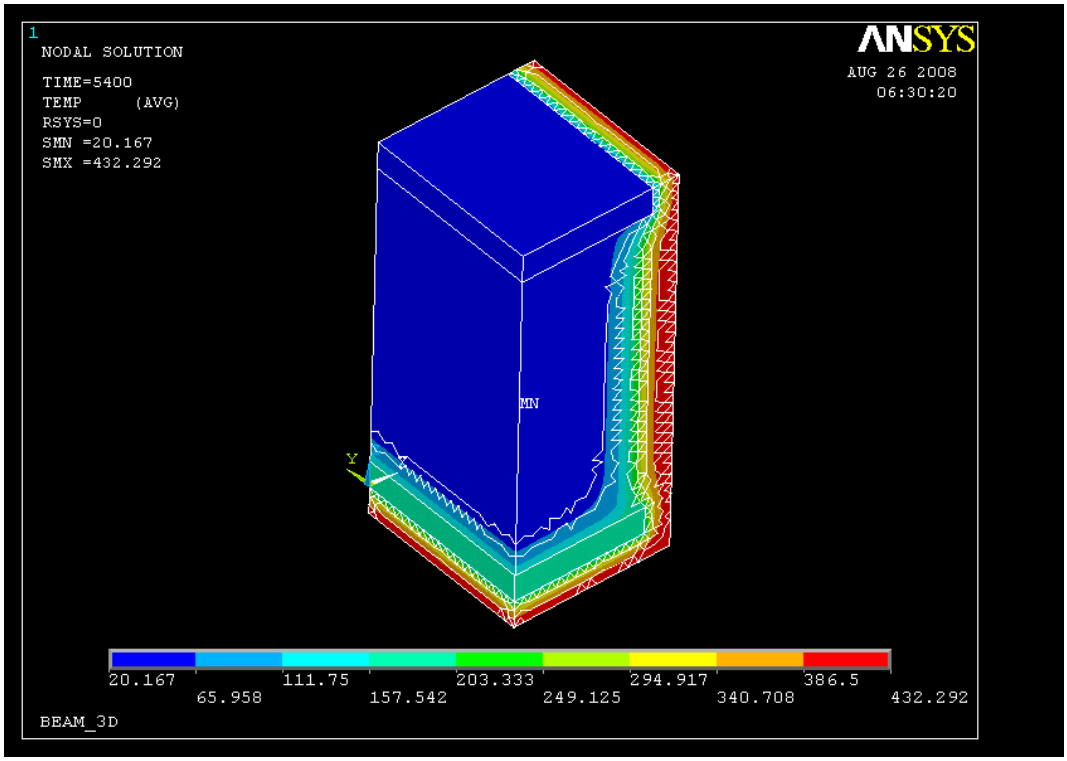

Figure 3.14: Temperature distribution at 5400[S]

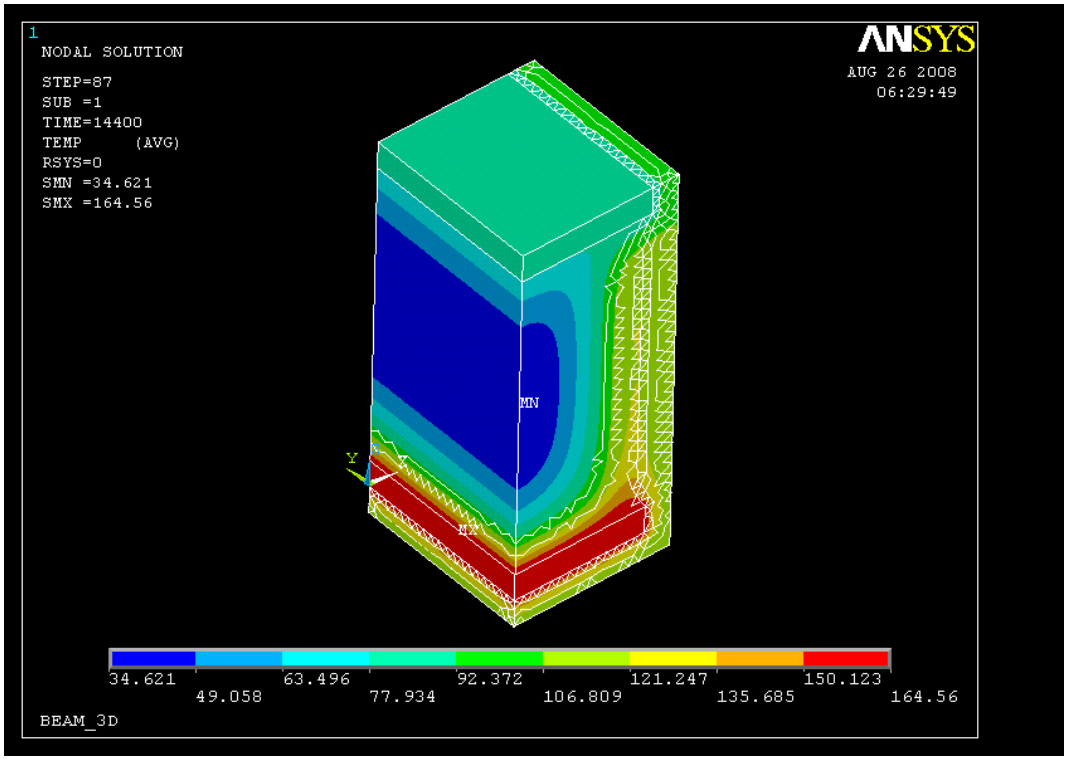

Figure 3.15: Temperature distribution at 14400[S]

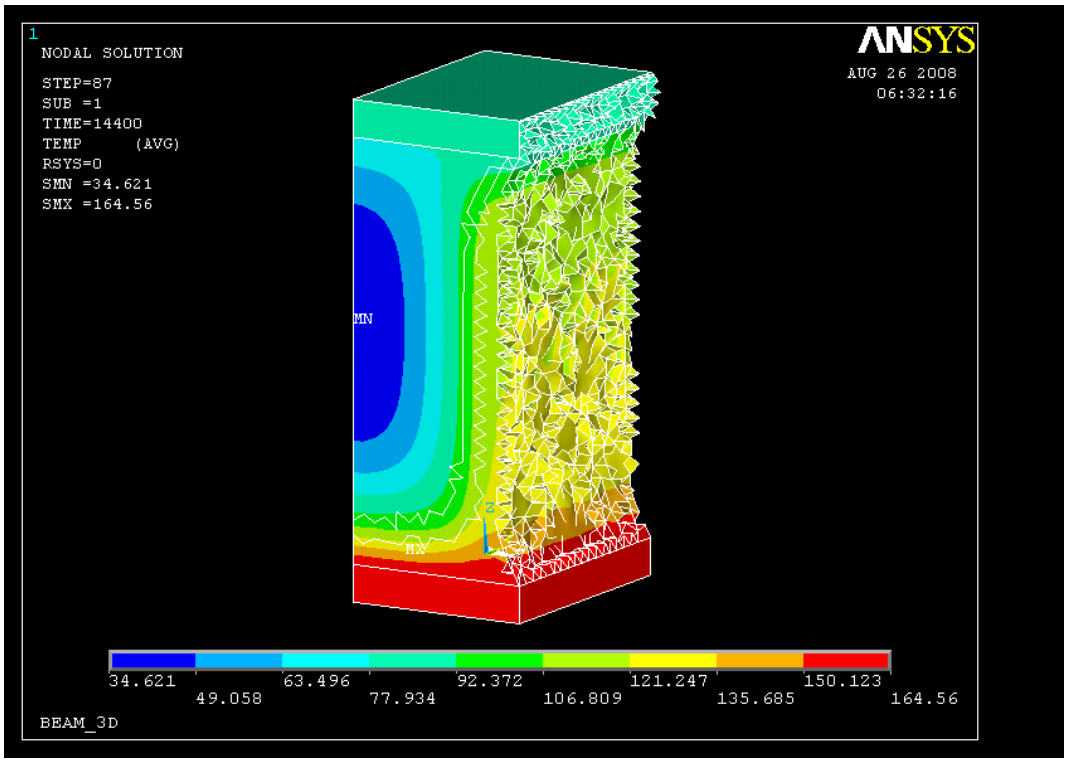

Figure 3.16: Remaining section at 14400[S]

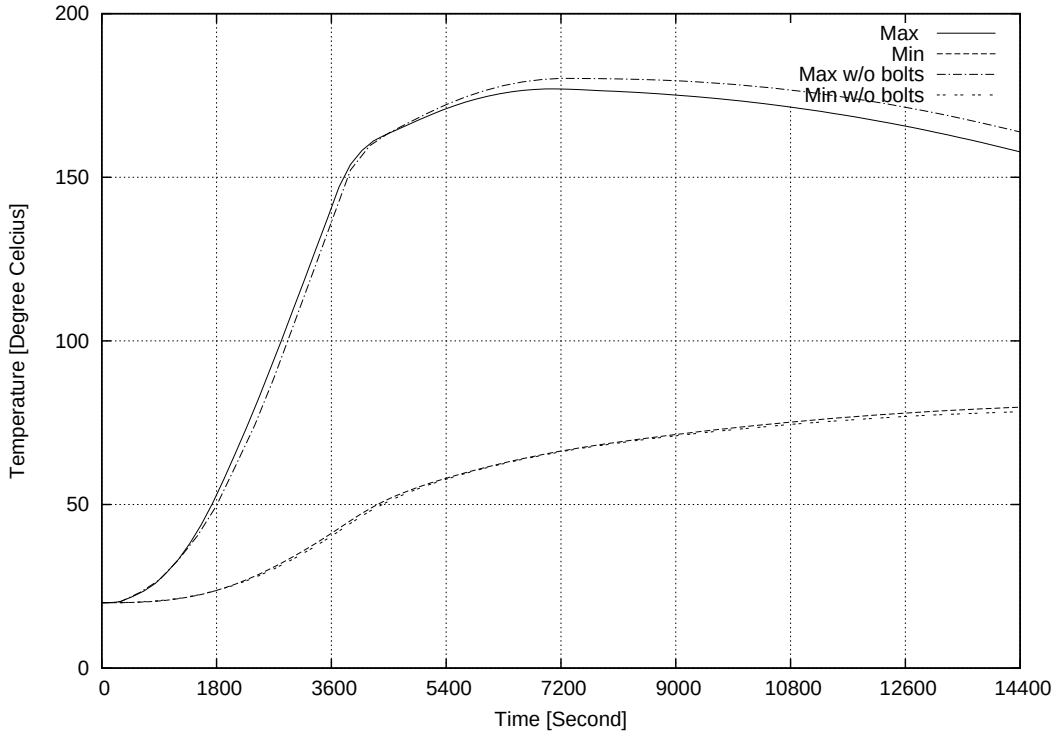

Figure 3.17: Comparison of steel temperature over time

Effect of connectors as thermal conductor

Figure 3.4.5 shows the comparison about maximum and minimum steel temperatures over time of 2 variants. The maximum temperature of variant 1 was 180.2 $°C$, while that of variant 2 was 176.9 $°C$. The minimum temperatures of variant 1 and 2 were 79.81 $°C$ and 78.33 $°C$, respectively. The number and size of the bolts were determined by minimal structural requirement at an ultimate limit state. It is concluded that with bolt type shear connectors, the section did not have enough capability to conduct and redistribute heat in the cross-section, since only slight influence has been observed through out the simulation from that whether the cross section has or does not have shear connectors. Therefore, it is recommended to design timber-steel sections by expecting only the improvement in heat capacity, and not the improved thermal conductivity.

Chapter 4

Structural development

4.1 Building overview

The imaginative design was carried out using the structural members whose structural and thermal properties were investigated in the previous chapter. Since one of the major advantages of timber-steel hybrid element lies in the point that it allows larger span compared to conventional solid element of timber, the target in building type was set to office space. The specifications of the building are shown in following.

Place	Imaginary	
Building type	Office building	
Scale	Building footprint	1031m^2
	Total floor area	9770m^2
	Number of stories	10 + penthouse
Finishing	Roof	Asphalt waterproofing, Concrete roofing
	Floor	Tile carpet
	Cladding	Aluminum curtain wall
Structure	Category	Timber-Steel hybrid structure
	Frame type	Two-dimensional frame structure
	Footing	Pile foundation

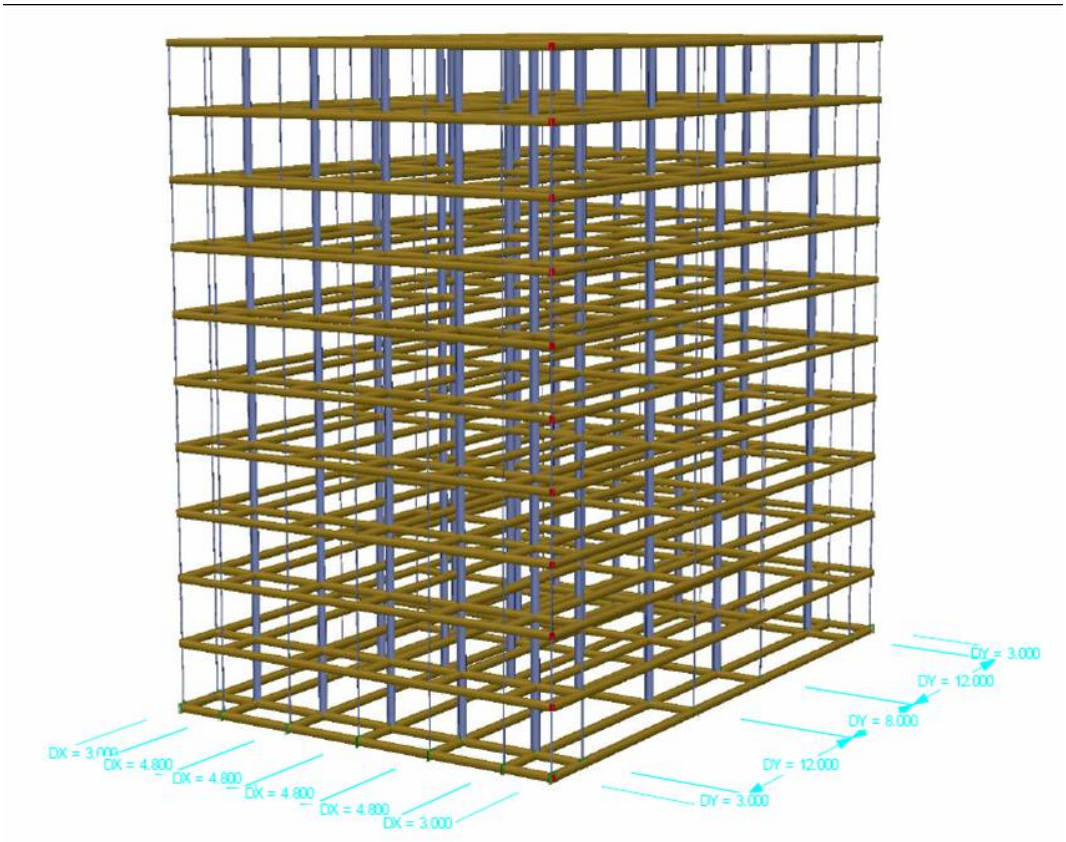

Figure 4.1: Building structure

4.2 Structural planning

4.2.1 Structural concept

1. The building is designed for the use of office with 10 stories. The structure has 25.2 m and 38 m in X- Y- direction, respectively. The common functions such as elevators, staircases, restrooms are designated in between Y3 and Y4 axes. The office spaces are assigned between Y2 and Y3 axes, and between Y4 and Y5 axes. The office space has the span of 12 m between perimeter zone and central zone, which contributes to forming universal and flexible office space.

2. As for the columns, timber-steel hybrid columns have been applied. The configuration of the column was the same as was proposed in [10] by the author. Outer rectangular timber surface and four steel plates inside have the angle of 45° derived from the disposition of the two materials where fire-thermal effects were considered. The amount of steel content varies according to the vertical position of each, and the dimension of outer surface does not vary.

3. Around the perimeter zone, a space with 3 m span was prepared. Structural point of view, the outer column with small dimension will contributes to building's horizontal stiffness against horizontal forces. Thermal condition of the office space inside was also considered using these widened perimeter zone.

4. As for the yielding mechanism, the design was made for the beams to reach the yielding mechanism earlier than the columns, except for the column top of the top story.

4.2.2 Elastic global analysis

Elastic global analysis was conducted following the load case below. The list of applied loads is in Table 4.1. Following assumptions were made:

a aaas

Load combination was developed by following EN 1990 [4]. The general form of load combination is as follows:

$$\sum (\gamma_{G,j} \cdot G_{k,j}) + \gamma_{Q,1} \cdot Q_{k,1} + \sum_{i>1} (\gamma_{Q,i} \cdot \psi_{0,i} \cdot Q_{k,i}) \tag{4.1}$$

The selected values for γ_G, γ_G and $\psi_{0,i}$ are listed in Table 4.2 and Table 4.3.

Table 4.1: Applied loads

Self Load G1	(variable by structural element)
Dead Load G2	
- Typical floor	
floor finishing	0.40 kN/m2
concrete	2.50 kN/m2
ceiling	0.30 kN/m2
- Roof floor	
finishing concrete	1.50 kN/m2
concrete	2.50 kN/m2
ceiling	0.30 kN/m2
Live Load Q1	3.0 kN/m2
Snow Load Q2	3.0 kN/m2
Wind Load Q3	q_0=0.80 kN/m2
Earthquake	lateral force

Table 4.2: Partial safety factor in EN 1990

	γ_F
Permanent load (G)	
-favorable	$\gamma_{G,inf} = 1.00$
-unfavorable	$\gamma_{G,sup} = 1.35$
Variable load (Q)	$\gamma_Q = 1.50$

Table 4.3: combination factor in EN 1990

variable load	ψ_0
live and traffic load:	
-office	0.70
Snow load	0.60
Wind load	0.60

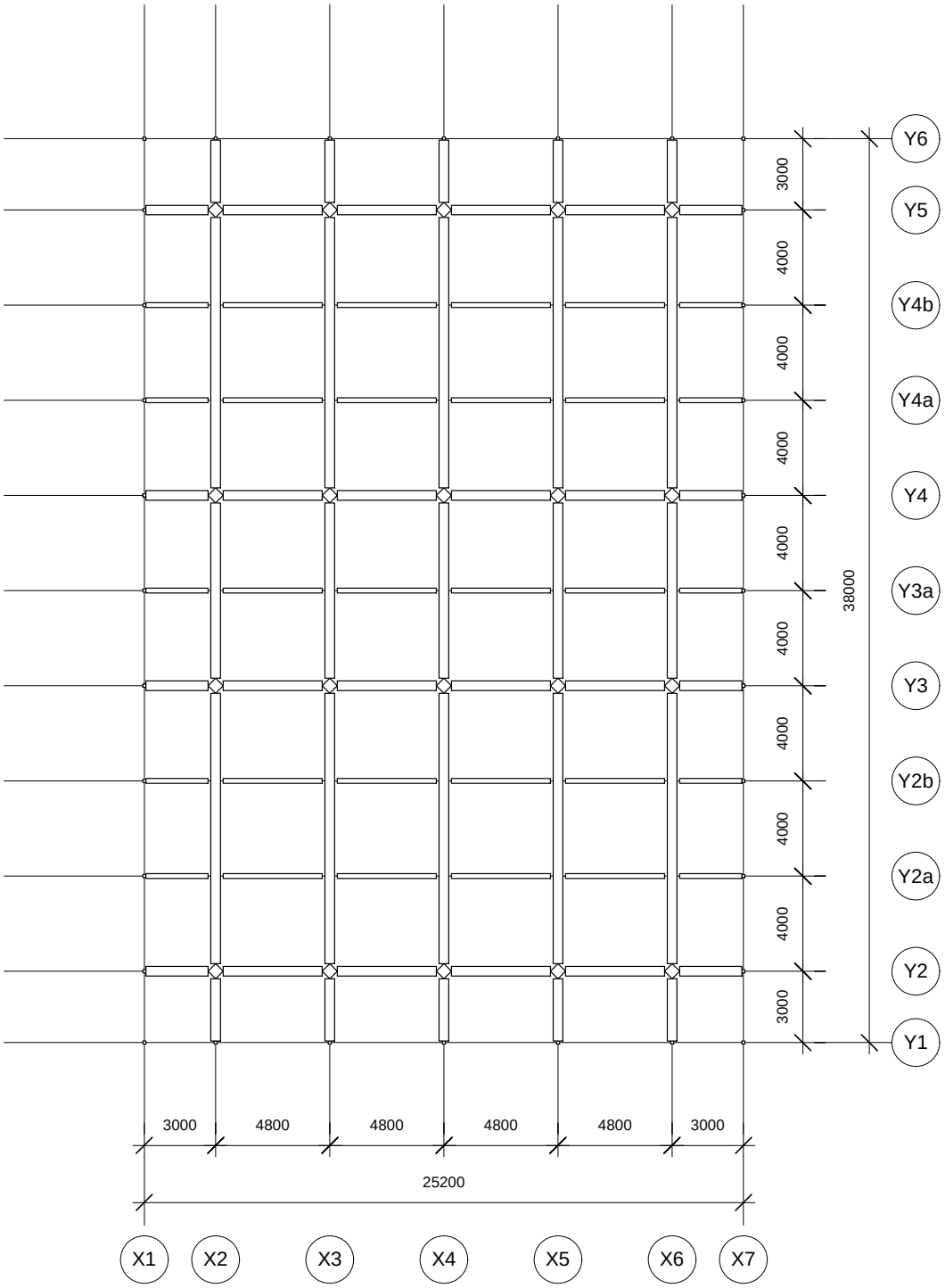

Figure 4.2: Structural Plan

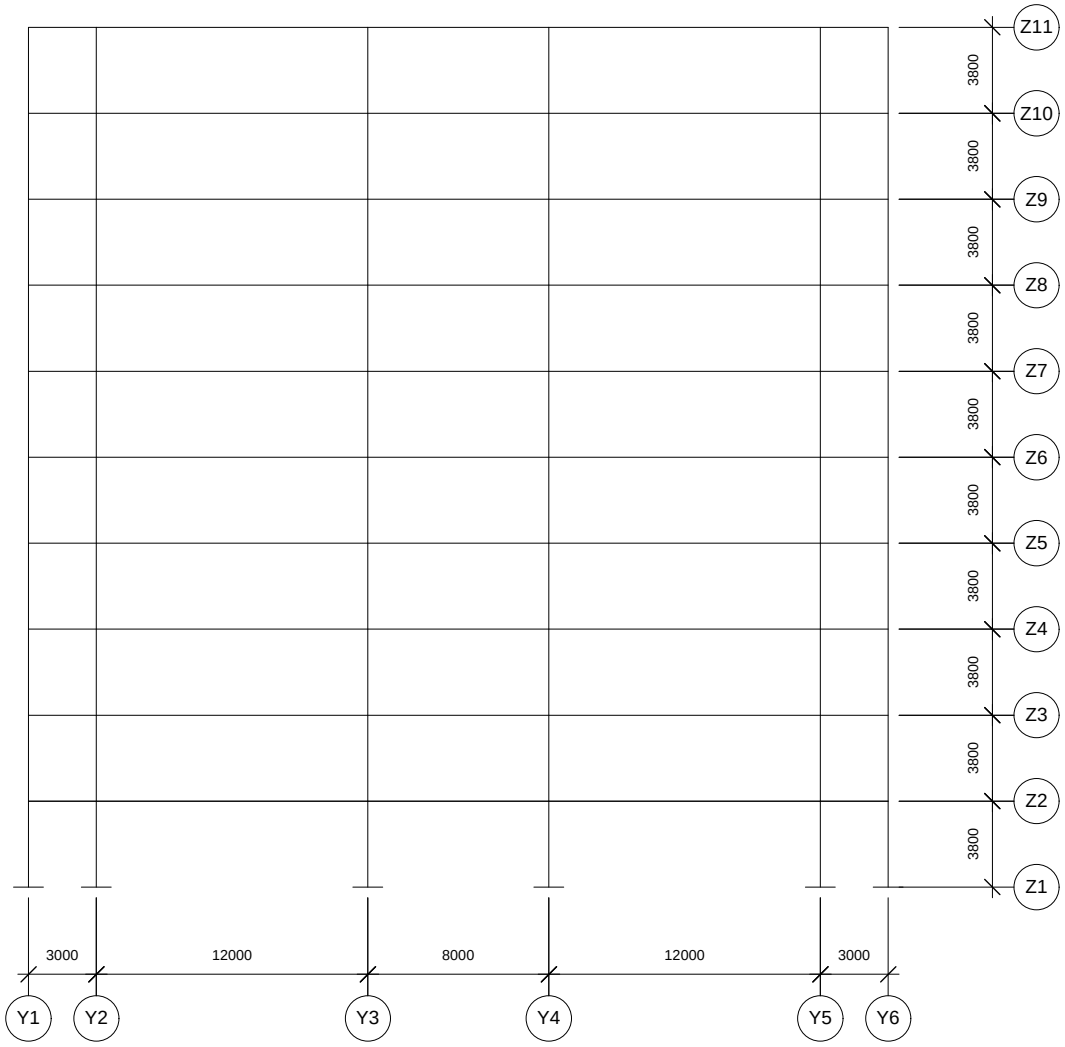

Figure 4.3: Structural section

4.2.3 Plastic analysis of the frame

Plastic frame analysis was conducted over two-dimensional frame as is shown in Figure 4.2.3. Seismic force was assumed to add to the structure as the horizontal force. The Japanese Building Standard Law [2] was respected for the plastic analysis of the seismic force.

The design load of seismic force is described as follows:

$$\text{Seismic force } Q_i = C_i \cdot \sum W_i \tag{4.2}$$

where,

$\sum W_i$: Total weight above story i

C_i : Story shear force at story i, $C_i = Z \cdot R_t \cdot A_i \cdot C_0$

Z : Regional factor (Reducing factor depending on region)
$0.7 \leq Z \leq 1.0$

R_t : Structural characteristic factor
(Reducing factor decided by characteristic period of the building)
$R_t = 1$ when $T \leq T_c$
$R_t = 1 - 0.2(T/T_c - 1)^2$ when $T_c \leq T \leq 2T_c$
$R_t = 1.6T_c/T$ when $2T_c \leq T$

T_c : Characteristic period of supporting ground
$0.4, 0.6,$ or 0.8 depending on the ground stiffness

T : Characteristic period for design
h : building height[m]

A_i : Distribution factor $A_i = 1/\sqrt{\alpha_i}$
$\alpha_i = \sum W_i / \sum W$

C_b : Standard shear coefficient $C_0 \geq 0.2$

$$\begin{aligned} \text{Building height } h &= 38\text{m} \\ \text{Characteristic period } T &= 1.189\text{[Hz]} \\ \text{Base shear coefficient } C_b &= 0.3 \\ \text{Regional factor } Z &= 1.0 \\ T_c = 0.6\text{[s]}, R_t &= 0.81 \end{aligned}$$

the weight of 1200 kN per each story was assumed in order to obtain the design story moment. The resultant values are calculated as are shown in Table 4.2.3.

The vertical load was assumed to work at the nodes and the enter of the beam elements, and each story has same vertical load. The following assumptions were made.

1. The distribution ratio of story moment is set initially 1 to 1, for column top and bottom, respectively.

2. Full plastic moment of the beam should be proportional to its length.

3. Plastic hinge should be made at the beam ends, and should not be at the center of a beam.

4. The proportion of bending strengths of column and beam r_{cb} is set to 1.5, except for the column top of top story and column base of ground story.

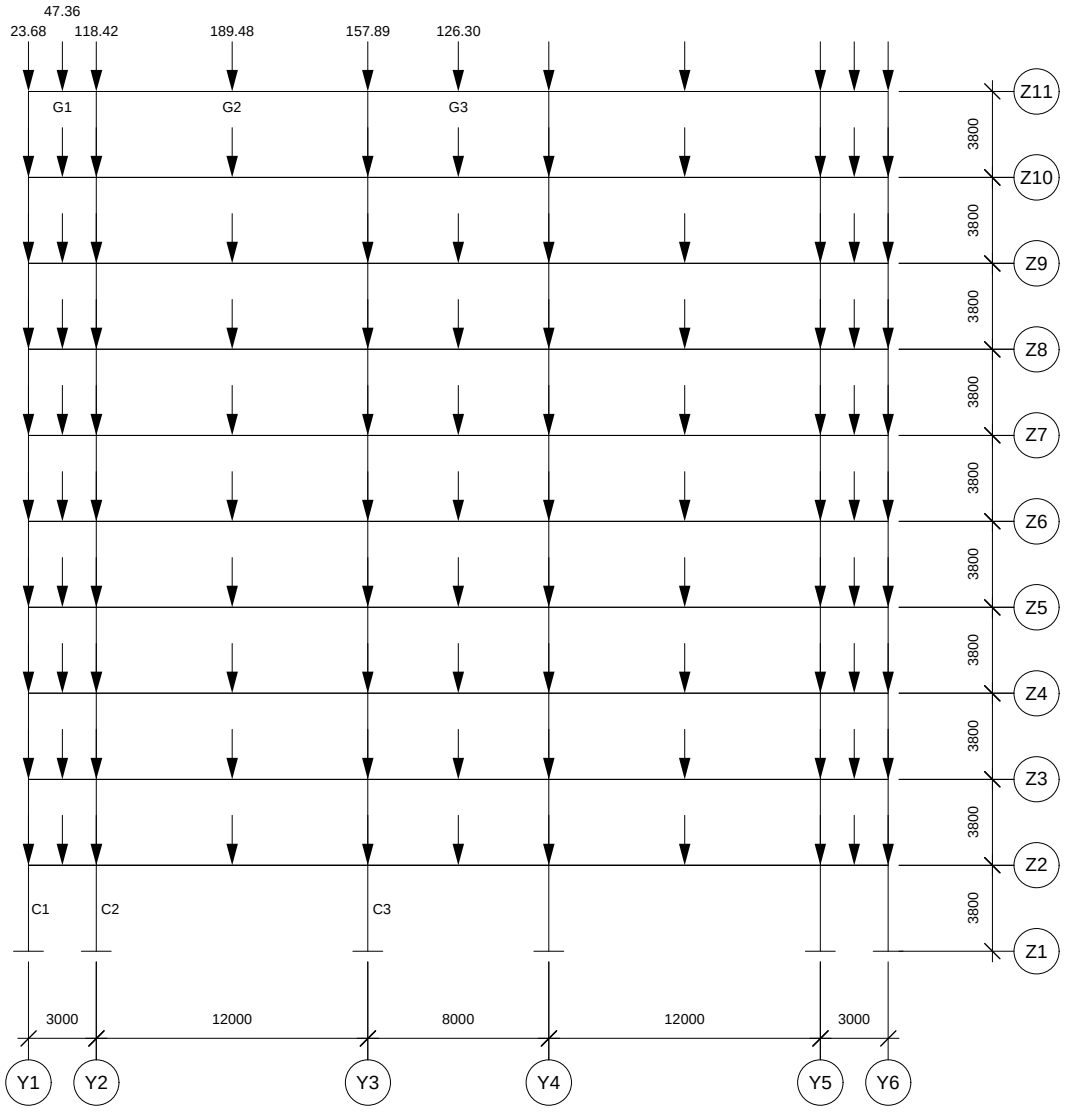

Figure 4.4: Design vertical load in KN

Table 4.4: Design value of story moment

Story	W_i [kN]	α_i	$\sqrt{\alpha_i}$	${}_sQ_i$ [kN]	${}_sM_i$ [kNm]
10	1200	0.1	0.32	1152	4378
09	2400	0.2	0.45	1610	6118
08	3600	0.3	0.55	1972	7493
07	4800	0.4	0.63	2277	8652
06	6000	0.5	0.71	2546	9673
05	7200	0.6	0.77	2789	10596
04	8400	0.7	0.84	3012	11446
03	9600	0.8	0.89	3220	12236
02	10800	0.9	0.95	3415	12978
01	12000	1.0	1.0	3600	13680

From the condition 2., the relationship among the full plastic moment of the beam G1 in Figure 4.2.3 $B_{i,1}$, of the beam G2 $B_{i,2}$, and of the beam G3 $B_{i,3}$ in the story i can be described as follows:

$$B_{i,2} = 4B_{i,1} \tag{4.3}$$

$$B_{i,3} = \frac{8}{3}B_{i,1} \tag{4.4}$$

Therefore:

$$\begin{aligned} {}_GM_i &= 4B_{i,1} + 4B_{i,2} + 2B_{i,3} && (4.5)\\ &= \frac{76}{3}B_{i,1} && (4.6)\\ &= \frac{19}{3}B_{i,2} && (4.7)\\ &= \frac{19}{2}B_{i,3} && (4.8) \end{aligned}$$

Condition 4. was set expecting columns to be in the realm of elasticity, in order to avoid the concentration of plastic hinge to a certain story. The column top of the top story and column base of ground story are excluded from this condition. In the ground story, the plastic hinges at the base of the column are assumed, therefore the distributed moment of the top and base of the column in the ground story is estimated according to the following equation, and Figure 4.2.3.

$${M_1}^T = \frac{1}{1 + r_{cb\,s}} M_1 \tag{4.9}$$

$${M_1}^B = \frac{r_{cb}}{1 + r_{cb\,s}} M_1 \tag{4.10}$$

From the Equation 4.3 and Equation 4.9, the bending moment of each column top and base can be obtained from the following equation:

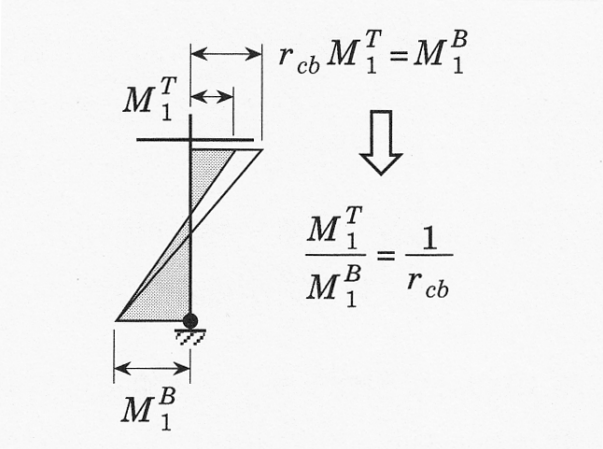

Figure 4.5: Distribution of story moment in the ground story.

$$C_i{}^B = \frac{M_i{}^B}{M_{i-1}{}^T + M_i{}^B}(B_1 + B_2) \tag{4.11}$$

$$C_{i-1}{}^T = \frac{M_{i-1}{}^T}{M_{i-1}{}^T + M_i{}^B}(B_1 + B_2) \tag{4.12}$$

The obtained result is shown in Table 4.2.3.

Table 4.5: Distribution of story moment and required plastic moments in kNm

Story i	${}_sM_i$	$M_i{}^T$	$M_i{}^B$	${}_GM_i$	$B_{i,1}$	$B_{i,2}$	$B_{i,3}$
10	4378	2189	2189	2189	86.4	345.6	230.4
09	6118	3059	3059	5248	207.2	828.6	552.4
08	7493	3746.5	3746.5	6801	268.5	1074	715.9
07	8652	4326	4326	8073	318.7	1275	849.8
06	9673	4836.5	4836.5	9163	361.7	1447	964.5
05	10596	5298	5298	10135	400.1	1600	1067
04	11446	5723	5723	11021	435.0	1740	1160
03	12236	6118	6118	11841	467.4	1870	1246
02	12978	6489	6489	12607	497.6	1991	1327
01	13680	5472	8208	11961	472.1	1889	1259

This result is used in Section 4.2.4

4.2.4 Section performance

Full plastic moment and maximal load bearing capacity

Figure 4.2.4 shows general stress-strain curve of timber under axial load. When the strength evaluation is made with small test pieces without knots or any defects, the

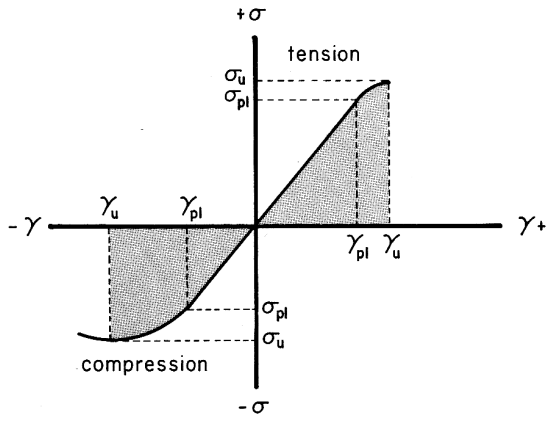

Figure 4.6: Stress-strain curve of timber, extracted from p.61, [1]

strength in tension is the strongest along the longitudinal direction, as is shown in Table 4.6. However, the influence of knots is dominant in decreasing the tensile strength with the real scale material with knots, and its value becomes generally less than bending strength[16] .

Table 4.6: Strength of zero defect specimen in N/mm^2, values extracted from [16]

	comp. propo. limit			comp. strength	tensile strength			shear strength	
species	L	R	T	L	L	R	T	R	T
Sugi	22.5	1.4	0.69	27.4	54.9	6.9	2.5	6.4	7.4
Silver Fir	27.4	1.9	1.2	34.3	108	7.8	3.4	9.8	8.3
Red Pine	27.4	2.5	1.8	40.2	127	9.3	3.9	10	11
Beech	31.4	3.5	2.2	48.0	108	18.1	8.8	12	15
Apitong	46.1	2.8	1.8	63.7	163	8.3	4.9	12	11

L: longitudinal direction, R: radial direction, T: tangential direction

For the structural calculation, the values from EN 1194 was chosen. The selected values are listed in Table 4.7. In principal, GL28 (glued laminated timber) class was selected for the building project.

Table 4.7: Characteristic value of strength in N/mm^2 [14]

	GL24		GL28		GL32		GL36	
	h	k	h	k	h	k	h	k
Bending $f_{m,g,k}$	24		28		32		36	
Tension parallel $f_{t,0,g,k}$	16.5	14	19.5	16.5	22.5	19.5	26	22.5
Tension perpendicular $f_{t,90,g,k}$	0.4	0.35	0.45	0.4	0.5	0.45	0.6	0.5
Compression parallel $f_{c,0,g,k}$	24	21	26.5	24	29	26.5	31	29
Compression perpendicular $f_{c,90,g,k}$	2.7	2.4	3.0	2.7	3.3	3.0	3.6	3.3
Shear $f_{v,g,k}$	2.7	2.2	3.2	2.7	3.8	3.2	4.3	3.8

full plastic moment of the composite

By using the required plastic moment which is in Table 4.2.3, the dimension of each member was decided. Axial force in the frame system is assumed to be small enough to be ignored. The required plastic moment for each member in i story is shown in Table 4.2.4.

Table 4.8: Required plastic moments in kNm

Story i	$B_{i,1}$	$B_{i,2}$	$B_{i,3}$
10	86.4	345.6	230.4
09	207.2	828.6	552.4
08	268.5	1074	715.9
07	318.7	1275	849.8
06	361.7	1447	964.5
05	400.1	1600	1067
04	435.0	1740	1160
03	467.4	1870	1246
02	497.6	1991	1327
01	472.1	1889	1259

When the joint area between column and beam is considered, it is better for all the beam elements to have the same height. Besides considering the construction, the less variants each element has, the easier and the more economical the construction becomes. Therefore 4 section types are proposed for the beam. The proposed sections are shown in Figure 4.2.4 to Figure 4.2.4.

Table 4.9: Required plastic moments in kNm and selected beam type

Story	G1			G2			G3		
i	$B_{i,1}$	${}_bM_p$	Type	$B_{i,2}$	${}_bM_p$	Type	$B_{i,3}$	${}_bM_p$	Type
10	86.4	626.0	50 A	345.6	626.0	50 A	230.4	626.0	50 A
09	207.2	626.0	50 A	828.6	1037	50 B	552.4	626.0	50 A
08	268.5	626.0	50 A	1074	1037	50 B	715.9	1037	50 B
07	318.7	626.0	50 A	1275	1480	50 C	849.8	1037	50 B
06	361.7	626.0	50 A	1447	1480	50 C	964.5	1037	50 B
05	400.1	626.0	50 A	1600	2167	50 D	1067	1037	50 B
04	435.0	626.0	50 A	1740	2167	50 D	1160	1480	50 C
03	467.4	626.0	50 A	1870	2167	50 D	1246	1480	50 C
02	497.6	626.0	50 A	1991	2167	50 D	1327	1480	50 C
01	472.1	626.0	50 A	1889	2167	50 D	1259	1480	50 C

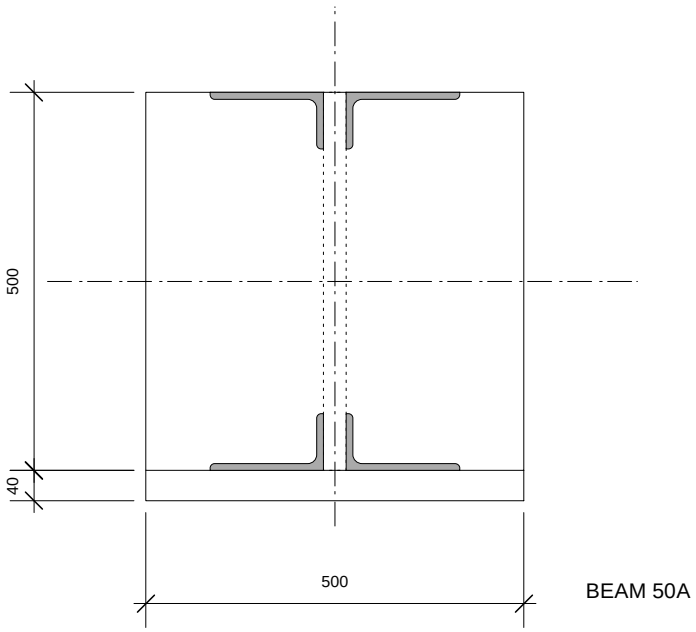

Figure 4.7: Beam section type 50A

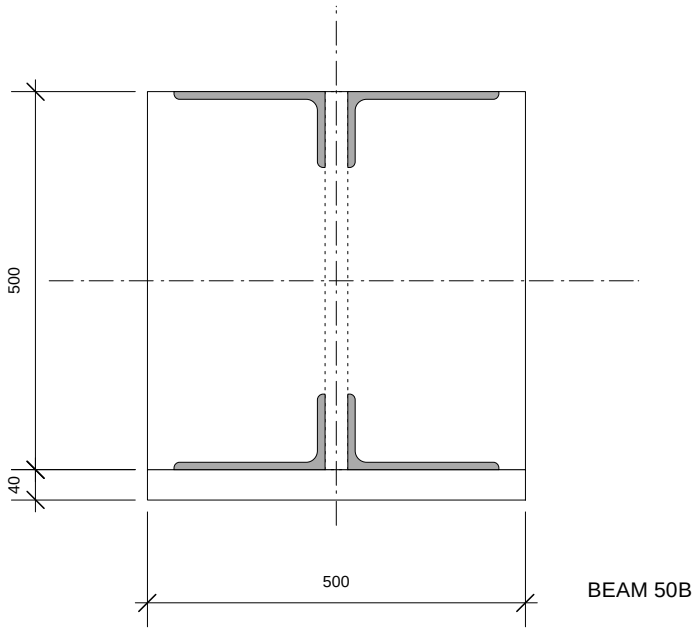

Figure 4.8: Beam section type 50B

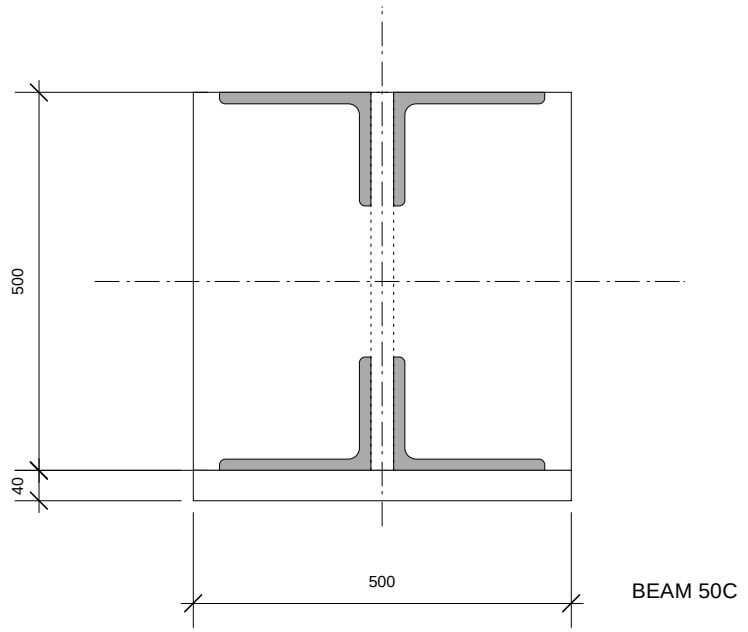

Figure 4.9: Beam section type 50C

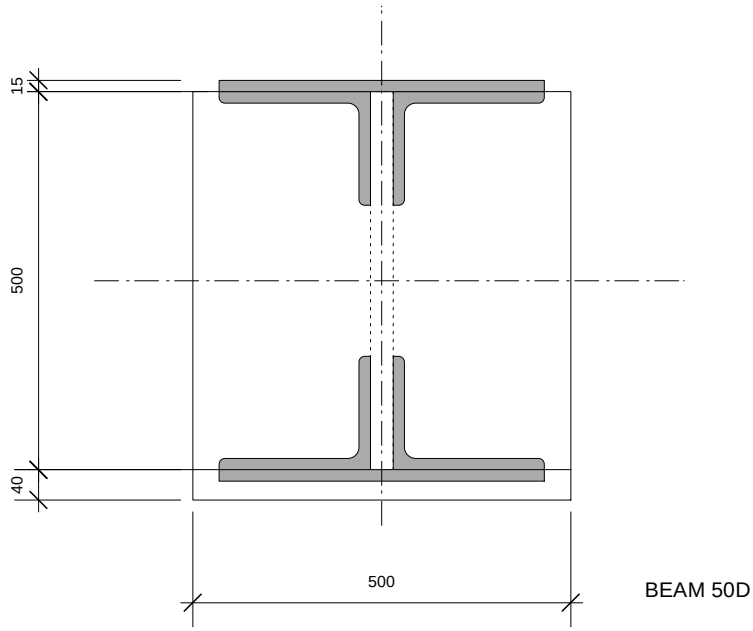

Figure 4.10: Beam section type 50D

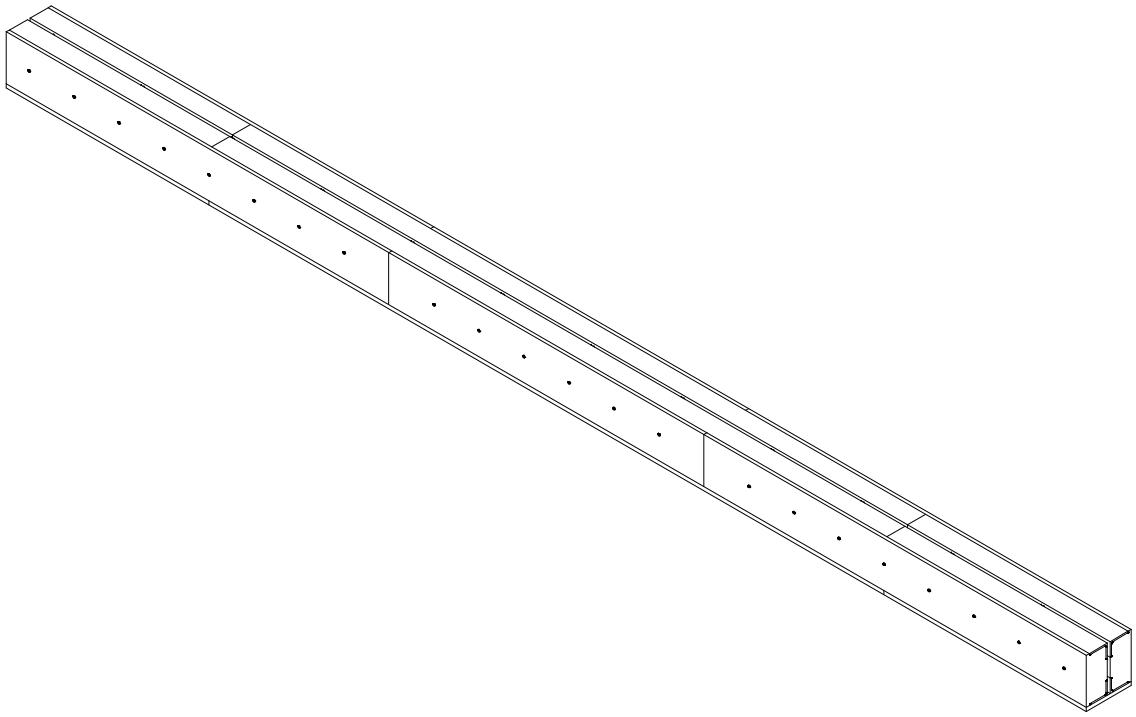

Figure 4.11: Beam construction

4.3 Detail design

Figure 4.3 and Figure 4.3 show the construction of the beam element, which is developed in this research. It was intended to have the connecting parts of timber-to-timber parts and steel-to-steel parts in different positions so that the beam element is assumed to be a contenuous element in the whole length.

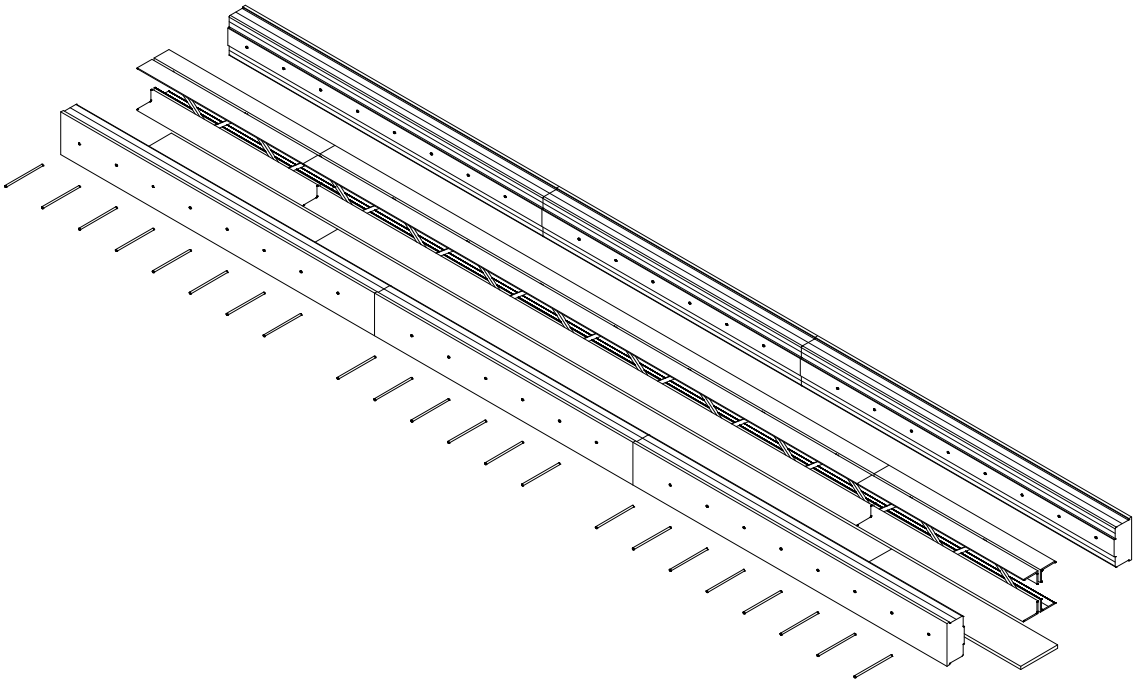

Figure 4.12: Beam construction

Chapter 5

Conclusion

5.1 Overview

Structural and thermal properties of a typical cross-section of wood-steel composite beam were surveyed. In the following sections, the achievements of this research are discussed.

5.2 Fire thermal topic

- Simplified method to evaluate the thermal capacity was proposed which uses density ρ and specific heat c and comparison was made between simplified method and two-dimensional thermal finite element analysis.

- Three dimensional thermal finite element analysis was conducted in order to survey the effect of shear connectors as a thermal conductor. Although slight effect has been observed, it has been found that bolt type shear connectors do not have sufficient capacity to transmit heat efficiently.

5.3 Structural development

- Structural global elastic analysis has been carried out for a timber-steel hybrid structure with ten stories.

- There are considerable improvement in moment of inertia, yield moment and full plastic moment of wood-steel composite. However, these properties are dominated by the methods of shear connectors between composite elements.

- By comparing the requirements for steel of thermal and structural properties, it has been found that thermal requirement is tighter than that of steel.

Bibliography

[1] Jozsef Bodig and Benjamin A. Jayne. *Mechanics of Wood and Wood Composites*. Van Nostrand Reinhold Publishing, 1982.

[2] The Building Center of Japan. *THE BUILDING STANDARD LAW OF JAPAN 2004*, 2004.

[3] C. Erchinger, A. Frangi, and A Mischler. Fire behaviour of multiple shear steel-to-timber connections with dowels. *Proceedings of the 38th CIB-W18 Meeting, University of Karlsruhe, Germany*, 2005.

[4] European Committee for Standardization. *EN 1990 Eurocode Eurocode - Basis of structural design*, 2002.

[5] European Committee for Standardization. *EN 1995-1-2 Eurocode 1: Actions on structures - Part 1-2: General actions - Actions on structures exposed to fire*, 2004.

[6] Andrea Frangi, Mario Fntana, and Markus Knobloch. Fire design concepts for tall timber buildings. *Structural Engineering International*, 2 2008.

[7] Jack.P. Holman. *Heat Transfer*. McGraw-hill, 9th edition, 2002.

[8] INFORMATIONSDIENST HOLZ. Brandschutzkonzepte fuer mehrgeschossige gebaeude und aufstockungen in holzbauweise. *HOLZABSATZFONDS Absatzfoerderungsfonds der deutschen Forst- und Holzwirtschaft*, 2005.

[9] Building Research Institute. Mokushitsu fukugou kenchiku kouzou gijutsu no kaihatsu, heisei 15 nendo houkokusho bouka bunkakai (in japanese, development of the technologies for timber composite structures, annual report in 2003), 3 2004.

[10] Bunji Izumi. Prototypentwicklung für mehrgeschossige öffentliche gebäude mit holz-stahl verbundkonstruktionen unter besondere berücksichtigung des brandverhaltens, 11 2007.

[11] Bunji Izumi, Yoshiaki Amino, Chi-Jen Chen, and Wolfgang Winter. Development of frame structures for multistory buildings with partial bending stiffness using timber-steel hybrid members with improved fire resistance. *Proceedings of 10th World Conference of Timber Engineering*, 6 2008.

[12] Knut Einar Larsen and Nils Marstein. *Conservation of Historic Timber Structures: An Ecological Approach*. Series in Conservation and Museology. Butterworth-Heinemann, elsevier edition, 5 2000.

[13] Hideo Oka, Hirokazu Ohashi, Jun ichi Yamaguchi, and Nagao Hori. A study on self-charring-stop of glued laminate timber made of japanese cedar installing mortar pieces. *Proceedings of 10th World Conference of Timber Engineering*, 6 2008.

[14] Proholz. *Bemessung in Holzbau, Von der nationalen zur europaeischen Normung*. Proholz Austria, 2002.

[15] Ian Smith and Andrea Frangi. Overview of design issues for tall timber buildings. *Structural Engineering International*, 2 2008.

[16] Hideo Sugiyama. *Mokushitsu Kouzou*. Kyoritsu Shupan, 3rd edition, 2002.

Affidavit

I, **BUNJI IZUMI** , hereby declare

1. that I am the sole author of the present Master Thesis, "Development of beam elements composed of timber and steel for medium-rise office buildings considering fire safety", pages, bound, and that I have not used any source or tool other than those referenced or any other illicit aid or tool, and
2. that I have not prior to this date submitted this Master Thesis as an examination paper in any form in Austria or abroad.

Vienna, _____ _____

Date Signature